

## RESEARCH ARTICLE

# Experimental analysis of the liquid-feeding mechanism of the butterfly *Pieris rapae*

 Seung Chul Lee<sup>1,2</sup>, Bo Heum Kim<sup>2</sup> and Sang Joon Lee<sup>1,2,\*</sup>
**ABSTRACT**

The butterfly *Pieris rapae* drinks liquid using a long proboscis. A high pressure gradient is induced in the proboscis when cibarial pump muscles contract. However, liquid feeding through the long proboscis poses a disadvantage of high flow resistance. Hence, butterflies may possess special features to compensate for this disadvantage and succeed in foraging. The main objective of this study is to analyze the liquid-feeding mechanism of butterflies. The systaltic motion of the cibarial pump organ was visualized using the synchrotron X-ray imaging technique. In addition, an ellipsoidal pump model was established based on synchrotron X-ray micro-computed tomography. To determine the relationship between the cyclic variation of the pump volume and the liquid-feeding flow, velocity fields of the intake flow at the tip of the proboscis were measured using micro-particle image velocimetry. Reynolds and Womersley numbers of liquid-feeding flow in the proboscis were ~1.40 and 0.129, respectively. The liquid-feeding flow could be characterized as a quasi-steady state laminar flow. Considering these results, we analyzed the dimensions of the feeding apparatus on the basis of minimum energy consumption during the liquid-feeding process. The relationship between the proboscis and the cibarial pump was determined when minimum energy consumption occurs. As a result, the volume of the cibarial pump is proportional to the cube of the radius of the proboscis. It seems that the liquid-feeding system of butterflies and other long-proboscid insects follow the cube relationship. The present results provide insights into the feeding strategies of liquid-feeding butterflies.

**KEY WORDS:** *Pieris rapae*, Biomechanics, Cibarial pump, Proboscis

**INTRODUCTION**

Butterflies mainly feed on liquids, such as floral nectar. These insects engage in active suction feeding, and a high pressure gradient is generated in their slender proboscis (Kim et al., 2011b). In previous studies, the nectar-feeding mechanism of a butterfly was investigated to understand its foraging behavior and interaction with plants (e.g. Daniel et al., 1989). In these studies, this liquid-feeding mechanism of butterflies was numerically simulated. In particular, the Hagen–Poiseuille relationship describes the volumetric intake flow rate  $\dot{Q}$  in terms of morphological parameters (inner radius of the proboscis  $r$ ; proboscis length  $l$ ), fluid property (viscosity  $\mu$ ) and driving force (pressure gradient  $\Delta p$ ):  $\dot{Q} = \pi r^4 \Delta p / (8\mu l)$  (May, 1985;

Pivnick and McNeil, 1985; Daniel et al., 1989; Kim et al., 2011b). In this equation, the relationship between  $\mu$  and feeding rate can be determined, and the optimal nectar concentrations for several butterfly species can be predicted (Daniel et al., 1989; Borrell and Krenn, 2006; Kim et al., 2011b).

In liquid feeding, butterflies use specific organs, such as the proboscis and cibarial pump, to extract nectar from flowers; however, these organs have not been investigated in detail in the context of fluid mechanics. Following the Hagen–Poiseuille equation, the flow rate is inversely proportional to the length of the proboscis. A butterfly may compensate for this disadvantage by developing a larger pump (Borrell and Krenn, 2006). The relative sizes of the food canal and the cibarial pump must be in tune to achieve the efficient nectar feeding (Kingsolver and Daniel, 1995). Butterflies should feed efficiently for successful foraging and survival. However, studies have rarely provided sufficient information regarding the strategies used by butterflies to improve liquid feeding with a long proboscis.

The purpose of the present study was to investigate the liquid-feeding strategy of butterflies. The liquid-feeding mechanism of butterflies was visualized *in vivo* to explain the complete process. Recently, temporal variations in intake flow at the tip of the proboscis were determined using the micro-particle image velocimetry (PIV) velocity-field measurement technique (Lee et al., 2014). The systaltic motion of the cibarial pump in the head was observed *in vivo* by synchrotron X-ray micro-imaging. The 3D morphological structure of the cibarial pump was also observed by synchrotron X-ray micro-computed tomography (CT). Considering these experimental observations, we developed an ellipsoidal pump model to estimate the intake flow rate in the proboscis. We also measured the flow characteristics of the intake flow using micro-PIV and synchrotron X-ray imaging techniques. Finally, we analyzed the dimensions of the cibarial pump and the proboscis in butterflies and other long-proboscid insects to determine the liquid-feeding strategy.

**RESULTS****Dynamic behavior of the pump system**

Fig. 1 depicts typical X-ray images of the temporal variation in volume of the cibarial pump in a liquid-feeding cycle. The volume of the pump chamber varies as a result of the vertical motion of the upper layer of the pump chamber, whereas the bottom layer remains almost fixed (Eastham and Eassa, 1955; Daniel et al., 1989). The feeding process is divided into two stages based on the movement of the upper layer: expansion and contraction (Eberhard and Krenn, 2005; Westneat et al., 2008). The top side of the pump is pulled upward dorsally to fill its chamber with liquid sucked through the proboscis during the expansion stage ranging from  $0.125P$  to  $0.750P$ , where  $P$  is the period of cyclic motion (Westneat et al., 2008). The inlet valve connecting the cibarial pump and the proboscis is open in this stage, whereas the outlet

<sup>1</sup>Department of Mechanical Engineering, Pohang University of Science and Technology, Pohang Gyeongbuk 790-784, Republic of Korea. <sup>2</sup>Center for Biofluid and Biomimic Research, Pohang University of Science and Technology, Pohang Gyeongbuk 790-784, Republic of Korea.

\*Author for correspondence (sjlee@postech.ac.kr)

**List of symbols and abbreviations**

CT	computed tomography
$D$	Dean number
$f$	feeding frequency
$H$	height
$l$	proboscis length
$P$	period of cyclic motion
$P_{cp}$	power required for the cibarial pump to transport liquid through the proboscis
PIV	particle image velocimetry
$P_p$	power output required for proboscis deployment
$P_{tot}$	total power consumption
$\dot{Q}$	volumetric intake flow rate
$\dot{q}$	planar intake flow rate
$\dot{q}_{max}$	maximum planar intake flow rate
$r$	inner radius of the proboscis
$R_c$	radius of the pump chamber
$Re$	Reynolds number
$St$	Strouhal number
$T$	period of the pumping process
$U$	average velocity
$V_c$	volume of the pump chamber
$V_{cp}$	volume of the cibarial pump
$V_{max}$	maximum pump volume
$V_{min}$	minimum pump volume
$Wo$	Womersley number
$\Delta p$	pressure gradient
$\mu$	viscosity
$\rho$	density

valve connected to the esophagus is closed. The inlet valve is closed and the top part of the organ is pushed downward ventrally to discharge liquid food to the posterior gut through the opened outlet valve in the ejection stage ranging from  $0.750P$  to  $1.000P$ .

Typical X-ray CT images showing the 3D morphological structure of the cibarial pump are included in Fig. 2. The frontal view of the 3D-reconstructed cibarial pump (Fig. 2B) resembles an ellipse. The lateral view of the cibarial pump at the expansion stage (Fig. 1C) is also elliptical. However, the horizontal cross-section of the pump shown in a dorsal view image (Fig. 2C) is circular. The cibarial pump of a butterfly can be considered as a systaltic ellipsoid based on the sectional observations. The pump volume is periodically changed by decreasing and increasing its height ( $H$ ), while the circular shape of the horizontal cross-section is maintained (Fig. 2D). The cibarial pump can be represented by the following ellipsoidal model:

$$V_c = \frac{4}{3}\pi R_c^2 H, \quad (1)$$

where  $V_c$  is the volume of the pump chamber and  $R_c$  is the radius of the pump chamber.

The physical dimensions of  $R_c$  and  $H$  are directly measured based on the X-ray images (Fig. 1). The variation in  $V_c$  is calculated based on the 2D boundaries of the pump system using Eqn 1. Fig. 3B shows the phasic variation in the ensemble-averaged pump volume of the five feeding cycles of four butterfly samples. A total of  $266 \pm 105$  ms is required to fully fill the pump chamber with liquid, and  $100 \pm 22$  ms is required to discharge the liquid to the esophagus. The variation in volume of the pump chamber shows a gradual linear expansion and a rapid contraction in a single pumping cycle. The maximum expansion and contraction volumes of the pump are  $46.8 \pm 10.7$  and  $22.4 \pm 2.5$  nl, respectively. The period of the pumping process ( $T$ ) is  $365 \pm 110$  ms long. During the contraction phase, the back flow from the pump toward the proboscis is nearly negligible because the outflow during the ejection stage is only 4% of the total intake flow. The intake volume can be estimated as  $V_{max} - V_{min}$ , where  $V_{max}$  and  $V_{min}$

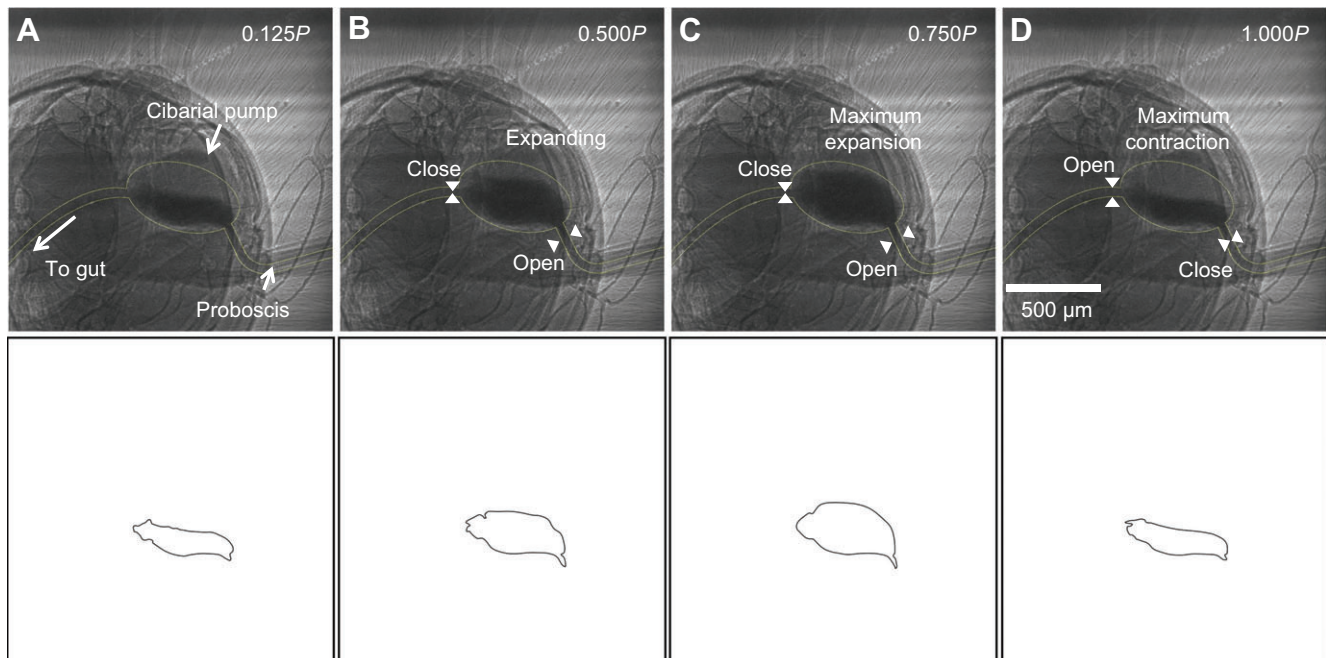


**Fig. 1. Typical X-ray images showing variation in a butterfly's pump organ and the corresponding variation in the pump chamber boundary.** Diluted iodine solution fed in the pump organ shows systaltic motion. Dotted yellow lines indicate the boundaries of the proboscis, cibarial pump, and esophagus. (A) The cibarial pump is contracted initially. (B,C) The top part of the pump organ is pulled dorsally upward to fill its chamber with liquid sucked through the proboscis. (D) The top part is pushed ventrally downward to discharge liquid food toward the posterior gut.  $P$  is the period of the cyclic liquid-feeding process;  $0P$  is the starting point of one cycle and  $1.000P$  is the end of the cyclic period.

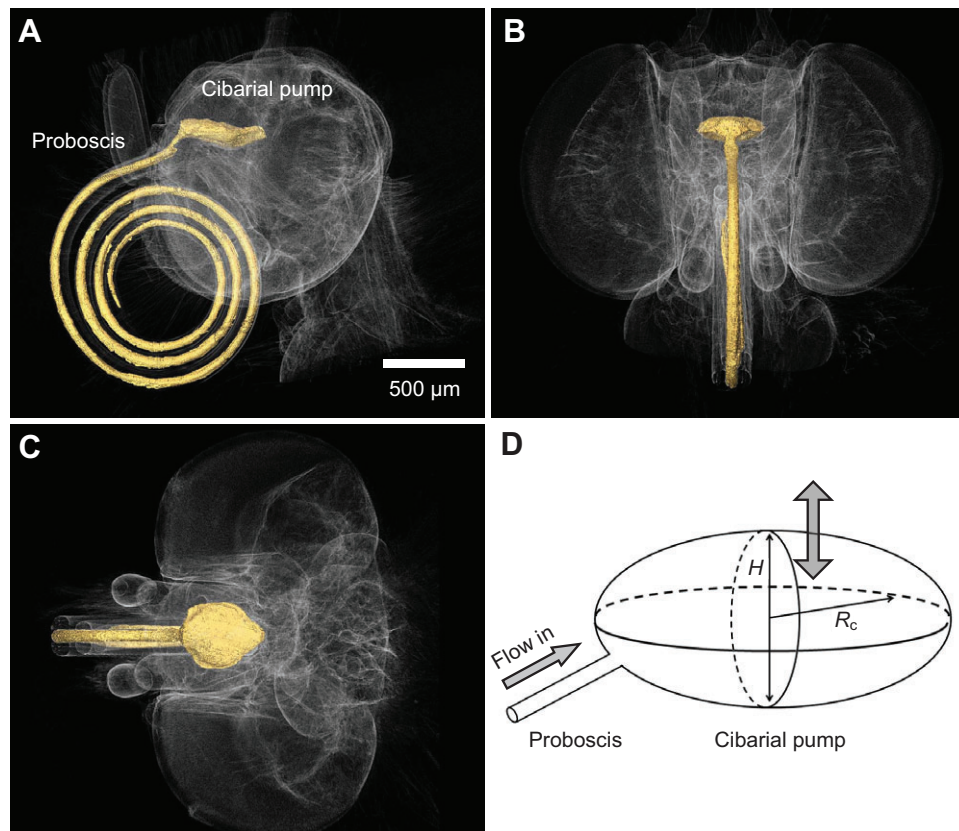


**Fig. 2. Three-dimensional reconstructions of a butterfly's head acquired by synchrotron X-ray micro-CT, and the corresponding model.** The feeding system (yellow) consists of a coiled proboscis and a cibarial pump. (A) Lateral view, (B) frontal view and (C) dorsal view. (D) An ellipsoidal model of the cibarial pump of a butterfly.  $H$ , height;  $R_c$ , radius of the pump chamber.

are the maximum and minimum volumes of the pump chamber at the end of the expansion and contraction stages, respectively. The intake flow rate ( $\dot{Q}$ ) can be calculated as follows:

$$\dot{Q} = \frac{V_{\max} - V_{\min}}{T} \quad (2)$$

The average intake volume flow rate is  $68.1 \pm 19.0 \text{ nl s}^{-1}$ . Table 1 shows the geometric dimensions and the ensemble-averaged liquid-feeding parameters obtained from the four butterfly samples used in this study.

### Liquid-feeding flow characteristics

The planar intake flow rates ( $\dot{q}$ ) measured using the micro-PIV technique show a pulsatile phasic variation as a result of the periodic systolic motion of the cibarial pump (Lee et al., 2014). Fig. 3A shows the temporal variation in the phase-averaged planar intake flow rate at the tip of the proboscis in one feeding cycle. The flow rate and time scale are normalized by the maximum planar flow rate ( $\dot{q}_{\max}$ ) and the corresponding feeding period (Lee et al., 2014). Flow can be divided into two distinct stages, namely, the intake and ejection stages, which indicate the expansion and contraction of the pump chamber, respectively. In the intake stage, liquid is sucked into the proboscis. In the short ejection stage, the proboscis discharges liquid outward. The amounts of the reversal flow and the total uptake flow were estimated by integrating the flow rate across the ejection stage and total duration, respectively (Fig. 3A). The amount of the reversal flow was found to be approximately 4% of the total intake flow (Lee et al., 2014).

Fig. 3B shows the variation in volume of the cibarial pump. The volume variations were ensemble averaged from four butterfly samples (Table 1). The liquid-feeding period measured by micro-PIV is 300 ms and that obtained from the synchrotron X-ray imaging technique is 365 ms. Therefore, the variation in the cibarial

pump was synchronized with the corresponding flow rate at the proboscis for analysis. The time period of the intake stage is almost similar to that of the expansion stage in the cibarial pump. In the initial part of the intake stage, the flow rate is remarkably increased and then it maintains the maximum value for a while. This phenomenon indicates the linear increase in the volume of the cibarial pump in the expansion stage (Fig. 3B). Based on these observations, we hypothesized that the proboscis works as a fluid-tight tube without leakage during the liquid-feeding process. In this study, the Reynolds number ( $Re$ ) based on the liquid-feeding flow inside the proboscis is  $\sim 1.40$ . This low Reynolds number indicates that the viscous effect is greater than the inertia force. Therefore, the curved proboscis and the slight irregularity in the conduit diameter slightly affect the liquid-feeding flow. In addition, the Dean number  $\{D = Re \sqrt{r/2(l/\pi)}\}$ , representing the centrifugal force effect of a curved channel, is  $\sim 0.092$ , where  $l$  is the length of the proboscis and  $r$  is the inner radius of the proboscis (Table 1). At this low value of the Dean number, the proboscis can be assumed to be a straight channel. Therefore, laminarity in flow is maintained (Kingsolver and Daniel, 1995). The Womersley number ( $Wo = r \sqrt{2\pi \rho / T \mu}$ , where  $\rho$  is density) is one of the most important parameters in pulsatile flow. In the present study, the Womersley number is  $\sim 0.129$ . The unsteady force is negligible and viscous effect is dominant when the Womersley number is  $< 1$ . Acceleration force is considered important in low Reynolds number flows when the time scale in velocity variation is short. The Strouhal number ( $St = fr/U$ , where  $f$  is the feeding frequency and  $U$  is the average velocity) is used to assess acceleration force; the acceleration force is negligible when the Strouhal number is  $< 1$  (Kingsolver and Daniel, 1995). In the present study, the Strouhal number is  $\sim 7.55 \times 10^{-3}$ . These non-dimensional parameter results indicate that the liquid-feeding flow inside the food canal is a quasi-steady laminar flow. Therefore, the

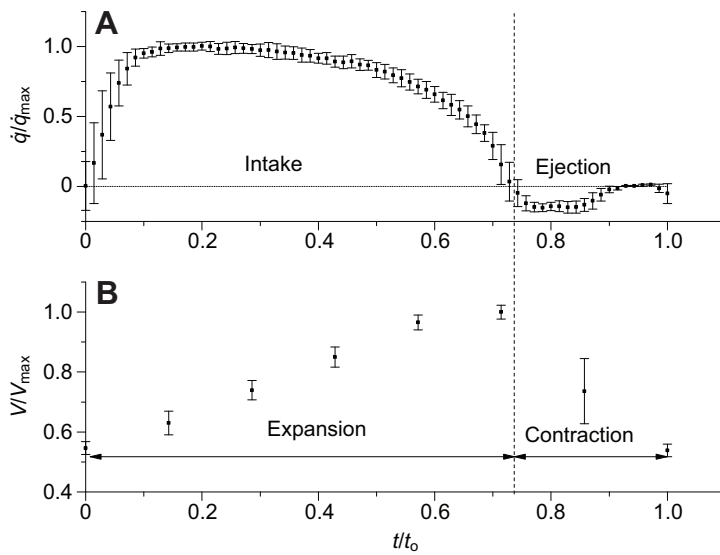


**Fig. 3. Variations in the planar intake flow rate and the volume of the cibarial pump.** (A) The planar intake flow rate variation around the tip of the proboscis acquired by micro-PIV measurement, and (B) the phasic volume variation of the cibarial pump acquired from synchrotron X-ray images. One feeding period is divided into two stages. The positive flow rate in the intake stage indicates that liquid is sucked into the proboscis. The negative flow rate in the ejection stage represents the flow disgorged from the proboscis (reversal flow). All data are expressed as means  $\pm$  s.d.  $\dot{q}/\dot{q}_{\max}$  denotes the normalized intake flow rate;  $V/V_{\max}$  is the normalized volume;  $t/t_0$  represents the nondimensional time normalized by the corresponding cyclic periods.

time-averaged flow inside the food canal is likely in accordance with the parabolic Hagen–Poiseuille relationship, although a short reverse flow is observed in the ejection stage (Lee et al., 2009).

**Liquid-feeding strategy of butterflies**

Considering that the Reynolds and Strouhal numbers of feeding flow inside the food canal have small values, the liquid-feeding strategy of butterflies can be analyzed based on the Hagen–Poiseuille relationship with geometrical simplification (Kingsolver and Daniel, 1995). In this analysis, we assumed that only the proboscis and the pump are involved in liquid feeding. A cibarial pump consumes energy for the intake of viscous liquid through the food canal. The power required for the cibarial pump to transport the liquid through the proboscis ( $P_{cp}$ ) can be estimated as follows:

$$P_{cp} = \Delta p \cdot \dot{Q} = \left[ \frac{8\mu l \dot{Q}}{\pi r^4} \right] \cdot \dot{Q}, \tag{3}$$

where  $\Delta p$  is the pressure gradient,  $\dot{Q}$  is the volumetric intake flow rate,  $\mu$  is the viscosity of the liquid, and  $l$  and  $r$  are the length and inner radius of the proboscis, respectively. Another source of power consumption is related to the deployment of the proboscis, which uncoils and straightens for probing nectar. The power output required for proboscis deployment ( $P_p$ ) depends on the cross-sectional area of the proboscis, which is proportional to  $r^2$ , so  $P_p \sim r^2$  (McMahon, 1973). Therefore, the total power consumption  $P_{tot}$  for liquid feeding can be expressed as follows:

$$P_{tot} = P_{cp} + P_p = A \frac{\dot{Q}^2}{r^4} + Br^2. \tag{4}$$

$P_{tot}$  is minimized when:

$$\frac{dP_{tot}}{dr} = -4A \frac{\dot{Q}^2}{r^5} + 2Br = 0 \tag{5}$$

and

$$\frac{d^2P_{tot}}{dr^2} = 20A \frac{\dot{Q}^2}{r^6} + 2B > 0. \tag{6}$$

Because  $A$  and  $B$  are positive constants, Eqn 6 is satisfied. Therefore, the minimum value of  $P_{tot}$  is derived when  $4A(\dot{Q}^2/r^5) = 2Br$ , so  $\dot{Q} \sim r^3$ . This relationship has the same form as Murray’s law (Zamir, 2000). The intake flow rate  $\dot{Q}$  can be estimated by the product of the feeding frequency  $f$  and the volume of the cibarial pump  $V_{cp}$ , so  $\dot{Q} \sim V_{cp} \times f$  (Lee et al., 2009). The feeding frequency is relatively constant based on the experimental results of Kim et al. (Kim et al., 2013), so  $\dot{Q} \sim V_{cp}$ . Therefore, the relationship between the radius and the volume of the cibarial pump is derived as  $r^3 \sim V_{cp}$ , when the minimum power consumption for feeding occurs. To check this tendency, we plotted  $V_{cp}$  against  $r$  on a log scale (Fig. 4A). The data were collected from experimental results of the test butterfly, *Pieris rapae*, and previous studies on liquid-feeding insects with a long proboscis. The slope is close to 3, supporting the proposed scaling. We also checked the relationship between the volumes of the proboscis,  $V_p$ , and the cibarial pump,  $V_{cp}$ .  $V_p$  would be proportional to the cube of its radius, so  $r^3 \sim V_p$ . Therefore,  $V_p$  may be proportional to  $V_c$ ,  $V_p \sim V_c$ , when  $P_{tot}$  is minimized. The volume of the proboscis and the cibarial pump evaluated from the X-ray tomography were approximately 0.0385 and 0.0252 mm<sup>3</sup>, respectively. These volumes at the same order of magnitude support the linear dependence.

**Table 1. Structural parameters of the proboscis and the dynamic liquid-feeding parameters of four butterfly samples obtained from the synchrotron X-ray imaging experiment**

Animal no.	$r$ ( $\mu$ m)	$l$ (mm)	$T$ (ms)	Expansion (ms)	Contraction (ms)	$V_{\max}$ (nl)	$V_{\min}$ (nl)	Flow rate (nl s <sup>-1</sup> )
1	29.5	10.9	240	167	73	44.9	23.7	88.3
2	33.7	11.4	347	223	124	34	19.3	42.4
3	30.6	11.7	367	260	107	48.3	21.7	72.3
4	30.0	10.9	507	413	94	60.1	25.0	69.2
Mean $\pm$ s.d.	31.0 $\pm$ 1.9	11.2 $\pm$ 0.4	365 $\pm$ 110	266 $\pm$ 105	100 $\pm$ 22	46.8 $\pm$ 10.7	22.4 $\pm$ 2.5	68.1 $\pm$ 19.0

The volume and flow rate information were obtained from the ellipsoidal model.

$r$ , radius;  $l$ , length of proboscis;  $T$ , total duration of a pump cycle;  $V_{\max}$ , volume of the cibarial pump when it is expanded to its maximum at the end of the intake stage;  $V_{\min}$ , volume of the cibarial pump when it is contracted to the minimum at the end of the ejection stage.

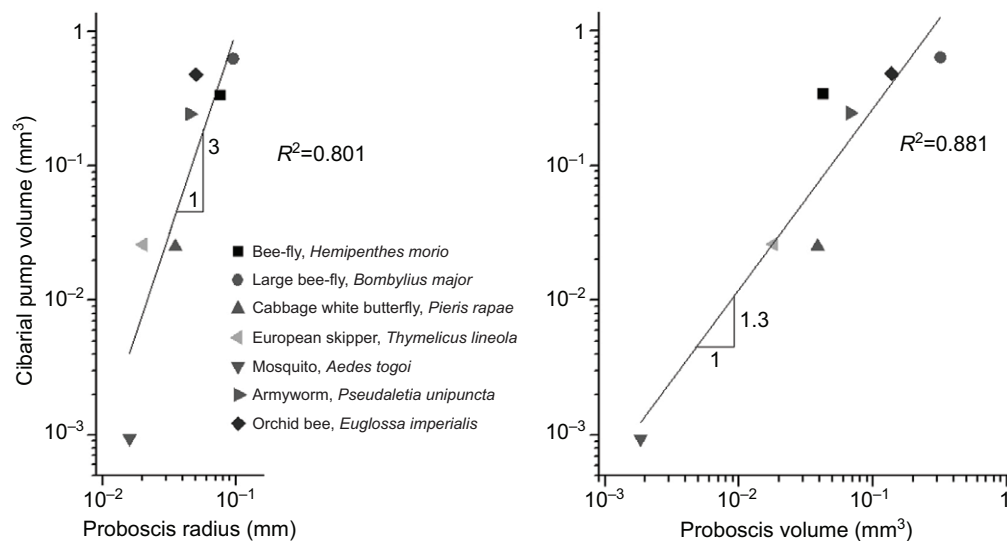


**Fig. 4. The dependence of the cibarial pump volume on the radius and volume of the proboscis.**

(A) Relationship between the volume of the cibarial pump and the radius of the proboscis. (B) Variation in the volume of the cibarial pump with respect to the volume of the proboscis. Data are shown on a log scale and were collected from the following sources: *Hemipenthes morio* (Szucsich and Krenn, 2002), *Bombylius major* (Szucsich and Krenn, 2002), *Thymelicus lineola* (Pivnick and McNeil, 1985), *Aedes togoi* (Lee et al., 2009), *Pseudaletia unipuncta* (Pivnick and McNeil, 1985), and *Euglossa imperialis* (Borrell, 2006).

Fig. 4B shows the relationships between the volumes of the cibarial pump and the proboscis. The slope is  $\sim 1.3$ . These results provide insights into the liquid-feeding strategy of long-proboscid insects.

## DISCUSSION

In this study, the liquid-feeding phenomena of butterflies were investigated experimentally using the synchrotron X-ray imaging and micro-PIV velocity field measurement techniques. These advanced imaging techniques have been recognized as effective for studying liquid-feeding insects (Westneat et al., 2008; Kikuchi and Mochizuki, 2011; Kim et al., 2011a; Monaenkova et al., 2012). We analyzed the dynamic motion of the cibarial pump and the corresponding ellipsoidal model. In addition, the feeding flow characteristics were determined to verify the assumption of a simple tube and Hagen–Poiseuille flow. Finally, we analyzed the liquid-feeding strategy from a biomechanical viewpoint.

There have been a few studies on the function of the cibarial pump. Eberhard and Krenn (Eberhard and Krenn, 2005) reported the systolic operation of the cibarial pump based on functional anatomy. They mentioned that the liquid-feeding cycle is composed of two phases: suction and swallow phases related to expansion and contraction of the cibarial pump, respectively. Westneat et al. (Westneat et al., 2008) observed the cibarial pump of a living butterfly using the synchrotron X-ray imaging technique. The results of these studies agree with those of the present study, although there is not detailed information about the volume and time scale of the previous studies. In the present study, the dynamic behaviors of the cibarial pump were observed consecutively during the liquid-feeding process. The liquid-feeding process consists of two stages: expansion and contraction. In the expansion stage, the cibarial pump is expanded linearly to the maximum volume when the cavity is filled with liquid from the proboscis. In the contraction stage, the pump is contracted rapidly to transport the liquid to the esophagus. The duration of the expansion stage is approximately 2.7 times longer than that of the contraction stage. It seems that the pump muscles are well developed for the contraction (Eastham and Eassa, 1955). In the present study, the test butterfly did not empty its cibarial pump completely after the contraction. The volume of the retained liquid after the contraction ( $V_{\min}$ ) was  $22.4 \pm 2.5$  nl,  $\sim 48\%$  of the maximum pump volume ( $V_{\max}$ ). If the cibarial pump is completely emptied, discontinuity occurs in the main flow coming from the proboscis toward the esophagus. It seems that butterflies

retain some amount of liquid for the next cycle. However, this aspect has not yet been studied in detail in the context of myology.

In a previous study on the modeling of the cibarial pump, Daniel et al. (Daniel et al., 1989) developed a cylindrical model based on anatomical observation. Their model assumed that the cylindrical pump has constant radius and the expansion state is caused by a change in height, somewhat similar to the model established in the present study. However, our elliptical model was based on the dynamic motions of live butterflies observed using a synchrotron X-ray imaging system.

It is difficult to estimate precisely the mechanism of the inlet and outlet valves of the pump from the X-ray images in this study. Therefore, we studied the opening and closing operation of the valves based on the boundary images of the cibarial pump (Fig. 1). The inlet valve located in front of the pump did not perfectly seal the discharged flow during the contraction phase, because a slight reversal flow occurred (Fig. 3A). However, the effect of imperfect sealing seems to be nearly negligible, because the reversal flow in the ejection stage was only 4% of the total intake flow (Lee et al., 2014). Therefore, the intake flow in the cibarial pumps is relatively well regulated by the valves located at the inlet and outlet of the pump system.

The flow around the tip of the proboscis and the volume change of the cibarial pump are similar in terms of time scale (Fig. 3). This implies that the expansion and contraction of the cibarial pump induce the intake and ejection stages, respectively. The intake flow exhibits large standard deviations at the beginning of the intake stage (Fig. 3A). This results from the dramatically increased intake flow rate in the initial stage. The initial rapid expansion seems to induce large fluctuations in the intake flow rate, although the standard deviations in the expansion stage are small (Fig. 3B). Likewise, the standard deviations of the volume in the contraction stage are relatively large because the volume decreased rapidly. However, these large standard deviations do not affect on the reversal flow in the ejection stage because it is regulated by inlet valve.

The liquid-feeding flow inside the proboscis has been considered as a quasi-steady state, laminar flow, because the Reynolds, Womersley and Strouhal numbers are estimated to be very small (Kingsolver and Daniel, 1995; Lee et al., 2009; Lee et al., 2014). In this study, we obtained those governing parameters under *in vivo* condition.

The liquid-feeding strategy of butterflies was investigated based on the Hagen–Poiseuille relationship in the present study. We

derived the relationship between the proboscis and the cibarial pump in terms of energy consumption. Minimum energy consumption may occur when the volume of the cibarial pump is proportional to the cube of the radius of the proboscis,  $r^3 \sim V_{cp}$ . The liquid-feeding organs of the test butterfly, *P. rapae*, seem to bear this cube relationship. We checked other insects having a cibarial pump with a long movable proboscis (Fig. 4). These insects are considered to have the same liquid-feeding mechanism as that of the butterfly in the viewpoint of fluid mechanics (Kim and Bush, 2012). These insects also follow the cube relationship. The present study thus provides insights into the liquid-feeding systems of butterflies and other long-proboscid insects. In addition, the experimental methodology employed in this study will be helpful for investigating the biomechanical aspects of liquid-feeding insects.

## MATERIALS AND METHODS

### Sample preparation

In this study, the cabbage white butterfly [*Pieris rapae* (Linnaeus 1758)] was selected as a test subject for observing liquid-feeding phenomena. It is the most common flower-visiting butterfly in the Republic of Korea. It has a well-developed proboscis and a cibarial pump for nectar feeding (Eastham and Eassa, 1955). Adult butterflies and pupae were bought from a merchant in Goyang, Republic of Korea. These butterflies were reared at 27°C with 80% relative humidity under 16 h:8 h light:dark condition. The butterflies were fed with artificial nectar using a cotton rod soaked in 10% sucrose. In this experiment, the butterflies were evaluated at 4 days post-emergence (Lee et al., 2009; Lee et al., 2014; Kim et al., 2011a; Kim et al., 2013).

The proboscis is typically coiled under a butterfly's head in a resting state. Therefore, the coiled proboscis was manually straightened using a slender needle to imitate the posture of liquid feeding. The straightened proboscis was then fixed using sticky tape. However, internal flow is hardly observed because the proboscis is opaque. As such, the uptake flow around the tip of the proboscis was measured using the micro-PIV technique. The straightened proboscis was then immersed in a test liquid to induce water intake (Lee et al., 2014).

The wings of live butterflies were laterally fixed on a two-axis stage to visualize the systaltic motion of the pump organs using the synchrotron X-ray imaging technique (Fig. 6A).

A test butterfly was decapitated, and the head was attached to the sample holder using instant glue to obtain the 3D morphological structures of the pump organs by synchrotron X-ray CT. After the test sample was mounted, the sample holder was placed in liquid nitrogen for a few seconds to freeze the head. The sample holder was then placed on a rotating stage, and cold nitrogen gas was supplied continuously using a cryojet to avoid dehydration after the sample was exposed to an X-ray beam (Kim et al., 2012).

### PIV measurement at the tip of the proboscis

A micro-PIV system was used to determine the characteristics of the temporal variations in intake flow during the liquid-feeding process. The micro-PIV

system comprises a vertical epi-fluorescence microscope (Eclipse 50i, Nikon, Tokyo, Japan), a continuous Nd:YAG laser ( $\lambda=532$  nm, SLOC, Shanghai, China) as a light source, a high-speed CMOS camera (Photron ultima APX, Fujimi, Tokyo, Japan), and a personal computer for data processing and control (Lee et al., 2009; Lee et al., 2014; Kim et al., 2011a; Kim et al., 2013). Fluorescent particles (Molecular Probes, Eugene, OR, USA) with a mean diameter of  $\sim 1.0$   $\mu\text{m}$  were mixed with DI water ( $\sim 2.5 \times 10^9$  beads  $\text{ml}^{-1}$ ) (Lee et al., 2014). These particles emit fluorescence at a peak wavelength of 554 nm after absorbing green light at a peak wavelength of 534 nm. The fluorescence images of the tracer particles were captured using a high-speed camera after passing an optical long-pass filter ( $\lambda=550$  nm). Clear fluorescent-particle images were obtained from the thin measurement plane by adjusting the depth-of-focus of the microscope (Meinhart et al., 1999; Lee et al., 2009). A 10 $\times$  objective lens with a numerical aperture of 0.25 was attached to the microscope to magnify the flow images. These flow images were recorded consecutively at a frame rate of 500 frames  $\text{s}^{-1}$ . A fast Fourier transform-based cross-correlation PIV algorithm was used to obtain instantaneous velocity field information from two consecutive flow images (Lee et al., 2009; Lee et al., 2014). Typical velocity vector fields obtained at the intake and ejection stages are depicted in Fig. 5. The intake flow rate ( $\dot{q}$ ) was evaluated by calculating the planar flow rate ( $\text{mm}^2 \text{s}^{-1}$ ), which was obtained by integrating the velocity data along the borderline 100  $\mu\text{m}$  away from the tip of the proboscis (Lee et al., 2014). The intake flow rates of five feeding cycle at the same phase angle were ensemble-averaged (Fig. 3A).

### Synchrotron X-ray imaging

The cibarial pump of a butterfly was visualized *in vivo* using the synchrotron X-ray micro-imaging system of the Pohang Accelerator Laboratory (PAL; Pohang, Republic of Korea). The 6C biomedical imaging (BMI) beamline provides monochromatic X-rays with energy at 10–60 keV (Kim et al., 2011a). The transmitting X-rays were converted to visible light by use of a scintillation crystal of  $\text{CdWO}_4$ , which was then reflected 90 deg by a gold-coated mirror and registered by a CCD camera (MegaPlusII ES2001, Redlake, Tallahassee, FL, USA) at a frame rate of 24 frames  $\text{s}^{-1}$ . The test butterflies ingested a diluted iopamidol solution (600  $\text{mg ml}^{-1}$ ; Fig. 6A). Iopamidol solution was used as a contrast agent in this study because the boundary of the pump chamber may not be clearly detected; this result could be attributed to the complicated anatomical structure of the cibarial pump chamber, which is covered with layers of muscles (Kim et al., 2011a). Fig. 1 shows typical X-ray images showing the volume variation of the cibarial pump in the corresponding feeding cycle (0–1P). The light intensity in the cibarial pump filled with the contrast medium was lower than that in the surrounding regions. Therefore, the boundary of the pump chamber is defined at the area where the intensity was remarkably changed (Fig. 1). ImageJ software was used to determine the edges in the captured X-ray images.

X-ray CT was applied to obtain the 3D morphological structure of the pump system of a butterfly. Fig. 6B shows a schematic of the synchrotron X-ray micro-CT system established at PAL. The test butterfly was decapitated, and the head was fixed on a rotating stage. The sample attached on the stage was rotated from 0 to 180 deg at intervals of 0.5 deg. A total of

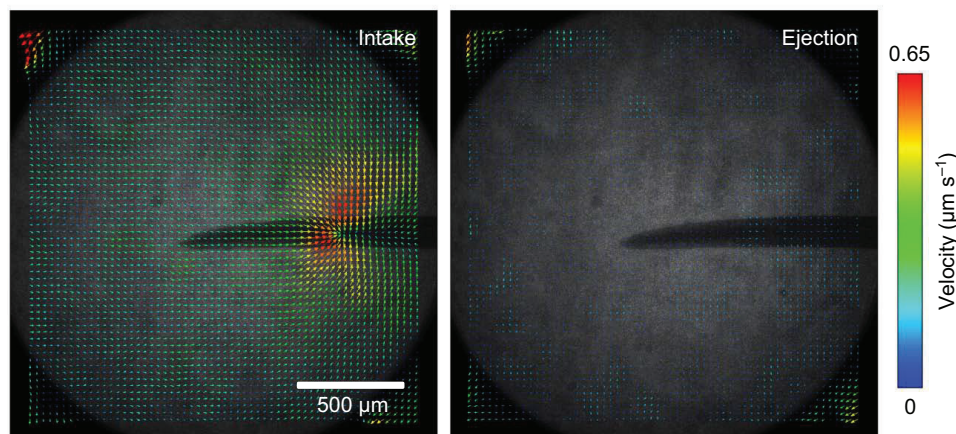


**Fig. 5. Typical velocity fields around the tip of the butterfly proboscis at the intake and ejection stages.**

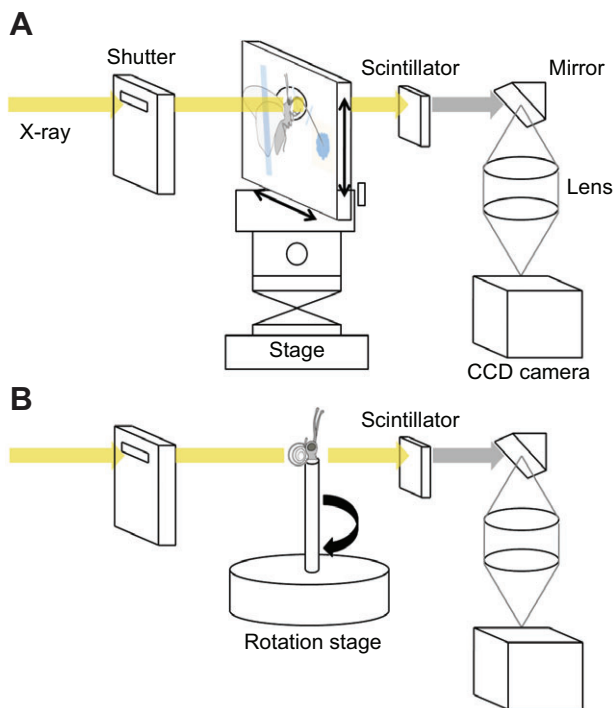


**Fig. 6. Schematic of the synchrotron X-ray micro-imaging technique.** A X-ray beam penetrating a test sample is converted to visible light after this beam passes through the scintillator. (A) Temporal variation in the pump organ of a butterfly was visualized *in vivo*. (B) The 3D morphological structure of a butterfly head was obtained by synchrotron X-ray micro-CT.

361 X-ray images were obtained using a CCD camera (VM-11M5, Vieworks, Gyeonggi-do, Republic of Korea). The 3D structure of the sample was numerically reconstructed from the projection slice images using the Octopus (in CT, Ghent, Belgium) image calculation program. Amira image analysis software (Visualization Sciences Group, Burlington, MA, USA) was used to analyze the 3D reconstructed images according to a previously described method (Kim et al., 2012).

#### Acknowledgements

Synchrotron X-ray imaging experiments were conducted at the 6C BMI beamline of the Pohang Accelerator Laboratory (PAL), Pohang, Republic of Korea.

#### Competing interests

The authors declare no competing financial interests.

#### Author contributions

S.C.L. designed and performed the experiments, analyzed the data and wrote the manuscript; B.H.K. designed and performed the experiments; S.J.L. designed the experiments, analyzed the data and wrote the manuscript.

#### Funding

This work was supported by the National Research Foundation of Korea (NRF) grant funded by the Korea government (MSIP) (no. 2008-0061991).

#### References

- Borrell, B. J. (2006). Mechanics of nectar feeding in the orchid bee *Euglossa imperialis*: pressure, viscosity and flow. *J. Exp. Biol.* **209**, 4901-4907.
- Borrell, B. J. and Krenn, H. W. (2006). Nectar feeding in long-proboscid insects. In *Ecology and Biomechanics: A Mechanical Approach to the Ecology of Animal and Plants* (ed. A. Herrel, T. Speck and N. Rowe), pp. 185-212. Boca Raton, FL: CRC Press.
- Daniel, T. L., Kingsolver, J. G. and Meyhöfer, E. (1989). Mechanical determinants of nectar-feeding energetics in butterflies: muscle mechanics, feeding geometry, and functional equivalence. *Oecologia* **79**, 66-75.
- Eastham, L. E. S. and Eassa, Y. E. E. (1955). The feeding mechanism of the butterfly *Pieris brassicae* L. *Philos. Trans. R. Soc. B* **239**, 1-43.
- Eberhard, S. H. and Krenn, H. W. (2005). Anatomy of the oral valve in nymphalid butterflies and a functional model for fluid uptake in Lepidoptera. *Zool. Anz.* **243**, 305-312.
- Kikuchi, K. and Mochizuki, O. (2011). Micro-PIV (micro particle image velocimetry) visualization of red blood cells (RBCs) sucked by a female mosquito. *Meas. Sci. Technol.* **22**, 064002.
- Kim, W. and Bush, J. W. M. (2012). Natural drinking strategies. *J. Fluid Mech.* **705**, 7-25.
- Kim, B. H., Kim, H. K. and Lee, S. J. (2011a). Experimental analysis of the blood-sucking mechanism of female mosquitoes. *J. Exp. Biol.* **214**, 1163-1169.
- Kim, W., Gilet, T. and Bush, J. W. M. (2011b). Optimal concentrations in nectar feeding. *Proc. Natl. Acad. Sci. USA* **108**, 16618-16621.
- Kim, B. H., Seo, E. S., Lim, J. H. and Lee, S. J. (2012). Synchrotron X-ray microscopic computed tomography of the pump system of a female mosquito. *Microsc. Res. Tech.* **75**, 1051-1058.
- Kim, B. H., Ha, H., Seo, E. S. and Lee, S. J. (2013). Effect of fluid viscosity on the liquid-feeding flow phenomena of a female mosquito. *J. Exp. Biol.* **216**, 952-959.
- Kingsolver, J. G. and Daniel, T. L. (1995). Mechanics of food handling by fluid-feeding insects. In *Regulatory Mechanism in Insect Feeding* (ed. R. F. Chapman and G. de Boer), pp. 32-73. New York, NY: Springer.
- Lee, S. J., Kim, B. H. and Lee, J. Y. (2009). Experimental study on the fluid mechanics of blood sucking in the proboscis of a female mosquito. *J. Biomech.* **42**, 857-864.
- Lee, S. J., Lee, S. C. and Kim, B. H. (2014). Liquid-intake flow around the tip of butterfly proboscis. *J. Theor. Biol.* **348**, 113-121.
- May, P. G. (1985). Nectar uptake rates and optimal nectar concentrations of two butterfly species. *Oecologia* **66**, 381-386.
- McMahon, T. (1973). Size and shape in biology. Elastic criteria impose limits on biological proportions, and consequently on metabolic rates. *Science* **179**, 1201-1204.
- Meinhart, C. D., Wereley, S. T. and Santiago, J. G. (1999). PIV measurements of a microchannel flow. *Exp. Fluids* **27**, 414-419.
- Monaenkova, D., Lehnert, M. S., Andrukh, T., Beard, C. E., Rubin, B., Tokarev, A., Lee, W. K., Adler, P. H. and Kornev, K. G. (2012). Butterfly proboscis: combining a drinking straw with a nanosponge facilitated diversification of feeding habits. *J. R. Soc. Interface* **9**, 720-726.
- Pivnick, K. A. and McNeil, J. N. (1985). Effects of nectar concentration on butterfly feeding: measured feeding rates for *Thymelicus lineola* (Lepidoptera: Hesperidae) and a general feeding model for adult Lepidoptera. *Oecologia* **66**, 226-237.
- Szucsich, N. U. and Krenn, H. W. (2002). Flies and concealed nectar sources: morphological innovations in the proboscis of Bombyliidae (Diptera). *Acta Zool.* **83**, 183-192.
- Westneat, M. W., Socha, J. J. and Lee, W. K. (2008). Advances in biological structure, function, and physiology using synchrotron X-ray imaging. *Annu. Rev. Physiol.* **70**, 119-142.
- Zamir, M. (2000). *The Physics of Pulsatile Flow*, pp. 49-50. New York, NY: Springer.